applied sciences

Communication

Power Quality Fault Identification Method Based on SDP and Convolutional Neural Network

Meng-Hui Wang, **Sheng-Hao Chi** and **Shiue-Der Lu** *

Department of Electrical Engineering, National Chin-Yi University of Technology, Taichung 411, Taiwan
* Correspondence: sdl@ncut.edu.tw; Tel.: +886-4-23924505 (ext. 7260)

Abstract: The global power demand is increasing year by year. Power quality fault recognition plays an important role in determining the fault type when a fault occurs, so as to maintain power quality and supply stability. Therefore, this paper proposed using the symmetrized dot pattern (SDP) algorithm plus the convolutional neural network (CNN) to study power quality fault recognition. Six common power quality fault models were taken as the subjects of discussion, including normal voltage, voltage sag, voltage swell, voltage interruptions, voltage flickers, and voltage harmonics. First, the voltage variation data of five cycles were extracted from a 60 Hz power supply and introduced into the SDP. Afterwards, the data were converted into graph data, which could be used for fault recognition. Lastly, the power quality fault type was identified by CNN. In this study, 600 random fault data (100 data per fault) were imported into the algorithm, and the recognition rate reached as high as 92.9%. Additionally, SDP could reduce the mass original data. After the subtle changes in the output signals were captured, they could be observed by images. The power quality fault state could thus be accurately recognized by CNN.

Keywords: power quality; symmetrized dot pattern; convolutional neural network

Citation: Wang, M.-H.; Chi, S.-H.; Lu, S.-D. Power Quality Fault Identification Method Based on SDP and Convolutional Neural Network. *Appl. Sci.* **2023**, *13*, 2265. https://doi.org/10.3390/app13042265

Academic Editor: Panagiotis G. Asteris

Received: 28 November 2022
Revised: 31 January 2023
Accepted: 8 February 2023
Published: 10 February 2023

1. Introduction

Under the rapid advancement of renewable energy, the emergence of artificial intelligence, the Internet of Things (IoT), and industrial upgrade to enter the high-tech industry, the current power systems contain numerous power and electronic equipment. The power systems are closely connected, and the voltage waveform is influenced by partial system faults or equipment switching, leading to transient variation and distortion of waveforms. This induces/results in power quality problems. The power supply stability is influenced, and the power equipment may fail. Therefore, the research on measurement analyses and fault recognition of power quality is quite important [1–3].

Traditionally, power quality measurement and analysis mostly use Fast Fourier Transform [4–6] to transform time-domain signals into frequency-domain signals to obtain the signal information in the frequency domain. However, this method only applies to processing steady-state and periodic signals. It cannot accurately display warning messages for other defective power quality problems. Based on S-transform and support vector machine (SVM), a method was developed to monitor and analyze power quality [7]. S-transform is a local time-frequency analysis method, which can simultaneously observe the energy distribution of signals in the time and frequency domains to extract the signal features and classify them using SVM. Ref. [8] proposed a method applicable to automated real-time monitoring of a one-phase power system. The mathematical morphology was combined with digital filtering to identify transient voltage. This method needs little/minimal calculation to identify the voltage state rapidly. However, this method cannot distinguish harmonics and interharmonics. Ref. [9] proposed a low-cost method for online monitoring and identifying the power quality and system disturbances induced by nonlinear loads. This method identifies different harmonic distortions based on THD of current and measurement of single harmonic components. Ref. [10] used the Google Image Search Engine to identify similar waveforms, classified the voltage and current waveform images, and provided information on possible faults. Ref. [11] developed a combined power quality automated recognition method based on Hilbert-Huang Transforms (HHT) and Relevance Vector Machine (RVM). The HHT can efficiently process harmonic signals and extract the features of power quality signals, whereas the RVM requires a large number of samples to perform classification and recognition according to power quality characteristics.

This study proposed a hybrid algorithm based on SDP and convolutional neural networks (CNN) for power quality fault recognition for rapid classification and recognition. Besides the signal of normal voltage, this study also included instantaneous signals of five common power quality accidents, such as voltage sag [12,13], voltage swell [13], voltage interruption [13], voltage flicker [14], and voltage harmonic [15] for experimental testing. First, a polar diagram was plotted based on the original power signal in the SDP for fault recognition [16–18]. Then, the CNN performed recognition to obtain the fault type. As the SDP was highly sensitive to input signals, a subtle change in the input signals is reflected in the output image. Meaningful eigenvalues can be extracted from the fault signals. Additionally, the proposed method was compared with HOG+SVM, HOG+Ensemble, and HOG+KNN to verify its accuracy.

2. System Architecture

Figure 1 shows the proposed method for signal analysis and recognition of power quality accidents. First, the original power signal was generated by MATLAB/Simulink. Then, the original power quality signal was transformed by SDP into a polar diagram with various image features. Afterward, the power quality accident signals were identified by CNN. The proposed algorithm is described below.

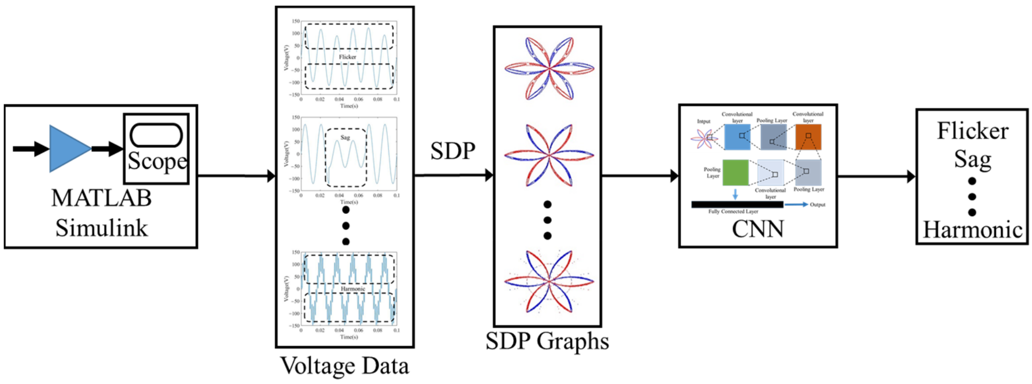

Figure 1. System architecture.

3. Symmetrized Dot Pattern

The SDP transforms the time-domain signals into a polar diagram through the data acquisition system. The patterns are compared to work out the differences. The principle is shown in Figure 2 [16–18]. Wherein r(i) is the radius of the polar diagram; θ(i) is the clockwise rotation angle of the x-axis; and Φ(i) is the counter-clockwise rotation angle of the x-axis.

$$\mathrm{r(i)} = \frac{\mathrm{X_i} - \mathrm{X_{min}}}{\mathrm{X_{max}} - \mathrm{X_{min}}} \tag{1}$$

$$\theta(\mathrm{i}) = \theta + \frac{\mathrm{X_{i+T}} - \mathrm{X_{min}}}{\mathrm{X_{max}} - \mathrm{X_{min}}} k \tag{2}$$

$$\Phi(\mathrm{i}) = \theta - \frac{\mathrm{X_{i+T}} - \mathrm{X_{min}}}{\mathrm{X_{max}} - \mathrm{X_{min}}} k \tag{3}$$

$X_{\max}$ in (1)~(3) is the maximum value of the original signal; $X_{\min}$ is the minimum value of the original signal; T is the signal interval time parameter ($1 \leq \mathrm{T} \leq 10$); θ is the initial deflection angle of the x-axis; k is the amplification coefficient of rotation angle ($k \leq \theta$).

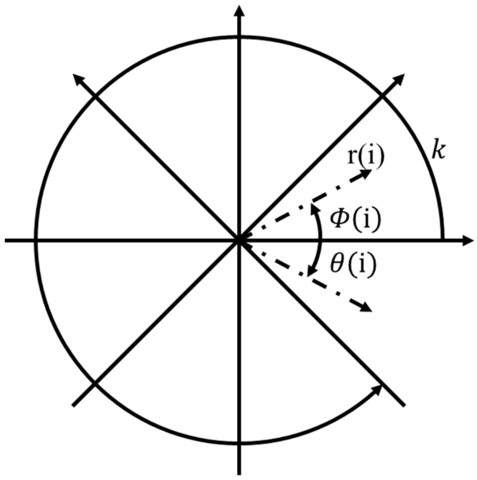

Figure 2. Schematic diagram of the SDP operation.

4. Convolutional Neural Network

With multiple layers, CNN can extract useful feature maps by transformation. It is a popular deep-learning neural network for image recognition functions [18], such as fast evaluation of transient voltage stability [19] and identifying the source of voltage sags [20]. The CNN architecture is shown in Figure 3, comprising the convolutional layers, pooling layer, and fully connected layer.

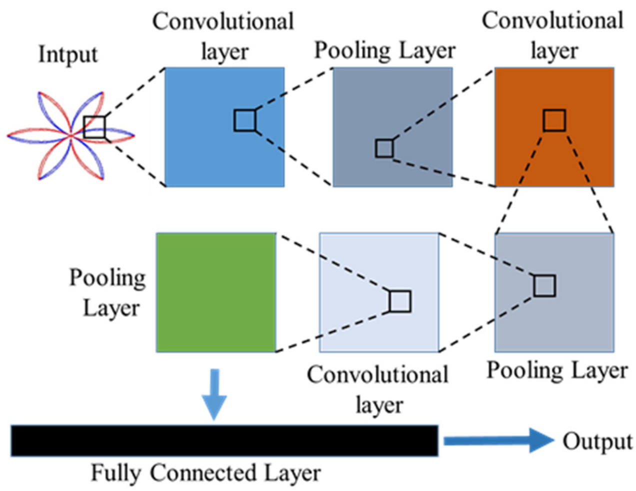

Figure 3. Schematic diagram of the CNN operation.

4.1. Convolutional Layer

The convolutional layers are used for feature extraction in the CNN. The convolution kernels of different sizes extract and enhance the features of patterns. The size of convolution kernels can influence the performance after feature extraction. If it is too small, the pattern feature recognition is poor. If it is too large, the computing time is too long. The calculation process is shown in Figure 4.

4.2. Pooling Layer

The pooling layer contains max pooling and average pooling. By compressing the image data, the most distinguished feature in the map can be seen. The pooling layer usually follows the convolutional layers to reduce the overall network computing complexity. It effectively reduces the extracted pattern feature parameter size and maintains the identity. As shown in Figure 5, the essential features of the original image can be maintained.

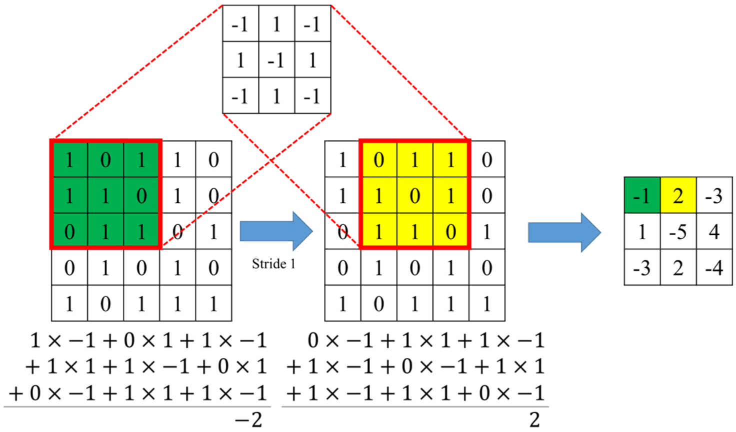

Figure 4. Schematic diagram of the convolutional layer operation.

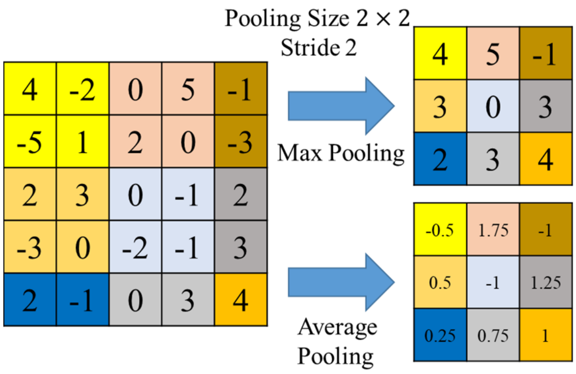

Figure 5. Schematic diagram of the pooling layer operation.

4.3. Fully Connected Layer

The main architecture includes the flatten, hidden, and output layers. Its effect is similar to a classifier. The error between input and output is modified by backpropagation, and the results obtained from the convolutional and pooling layers are predicted. The differences among different features can be identified better by changing the weight of each fully connected layer so that CNN can learn more complex feature combinations. The architecture is shown in Figure 6.

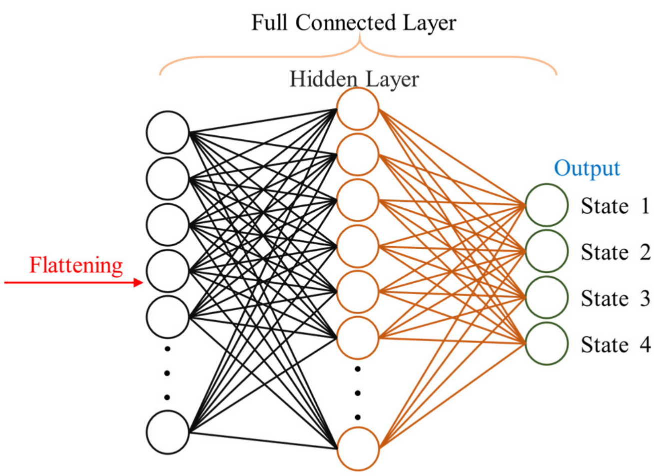

Figure 6. Schematic diagram of the fully connected layer operation.

5. Results

5.1. Power Analysis Data

Based on the literature [12–15], this study used MATLAB/Simulink to construct a power quality accident simulation circuit on the signals of power quality accidents and to generate the required accident waveform signal types. This includes voltage interruption, voltage swell, voltage sag, voltage flicker, and voltage harmonic. Each fault type had 100 pieces of data, and there were 600 pieces of data in total. Among them, 80 pieces of data of each fault type were used for training, and 20 pieces of data were for testing. Figure 7A–F shows the voltage signal waveform of one datum of various accidents.

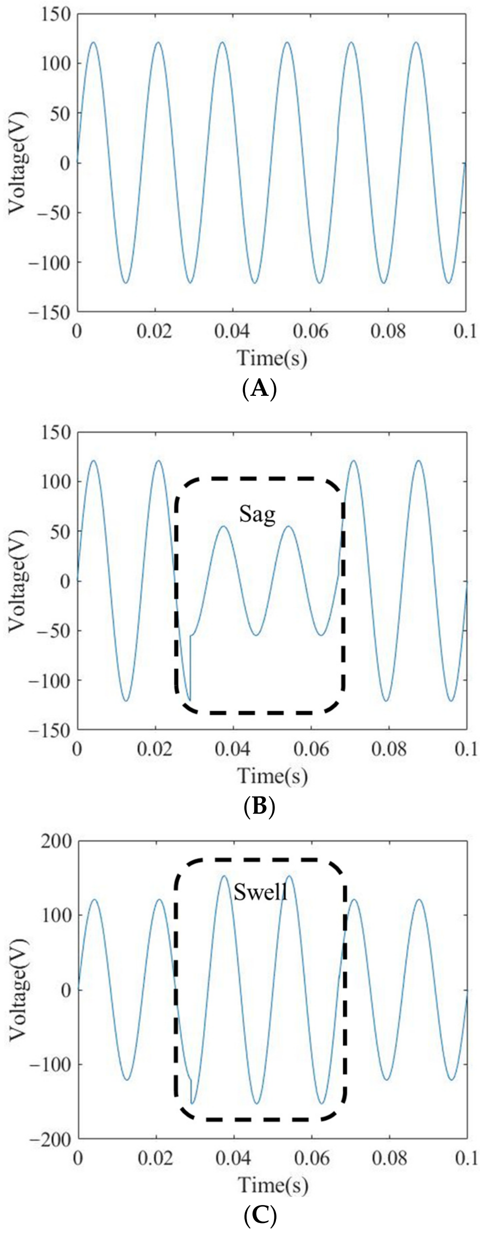

Figure 7. *Cont.*

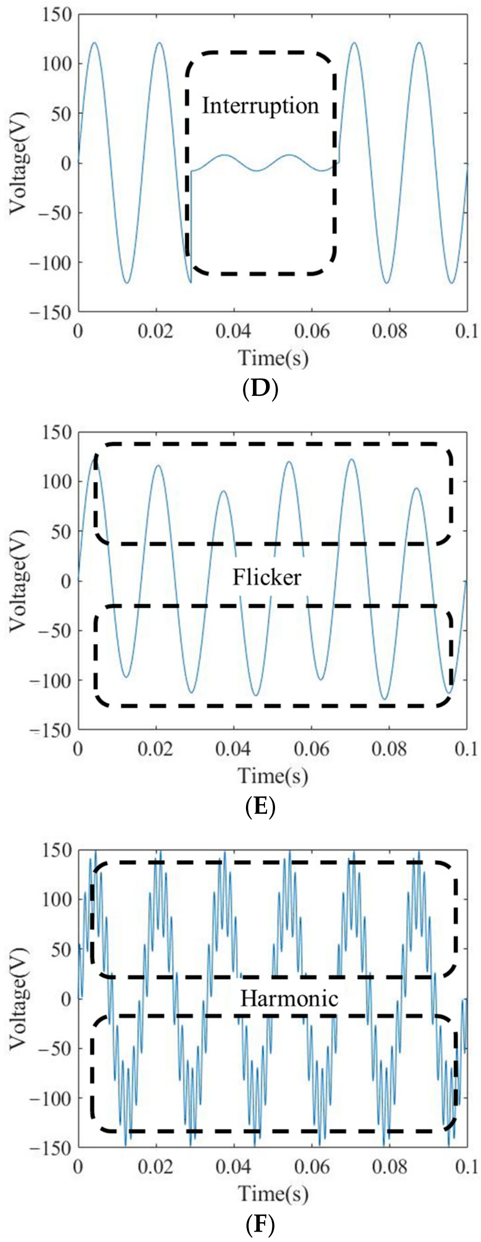

Figure 7. (**A**) Normal voltage. (**B**) Sag of voltage signals to 55 V during 0.029~0.067 s. (**C**) Voltage swell of voltage signals to 152.57 V during 0.029~0.067 s. (**D**) Interruption of voltage signals to 8.03 V during 0.029~0.067 s. (**E**) Flicker phenomenon of voltage signals. (**F**) Harmonic distortions of voltage signals.

5.2. Characteristic Signal Capture

Using the proposed extraction method, this study generated a snowflake diagram from the normal power signals through SDP, highlighting the features of power quality accidents. The power quality accident signals in Figure 7A–F were calculated by SDP. The obtained characteristic snowflake diagrams are shown in Figure 8A–F. The feature maps clearly show different distributions of power quality accident signals. This verifies that the proposed method could extract the power quality accident eigenvalues effectively.

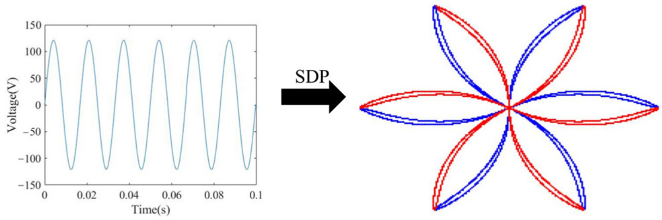

(**A**)

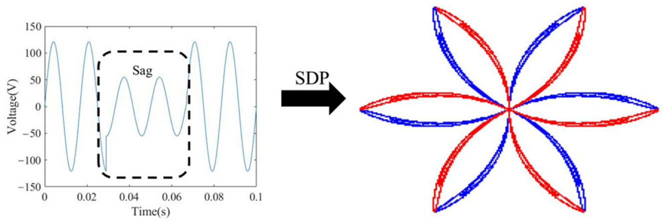

(**B**)

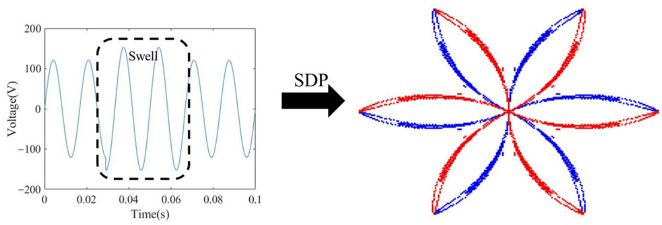

(**C**)

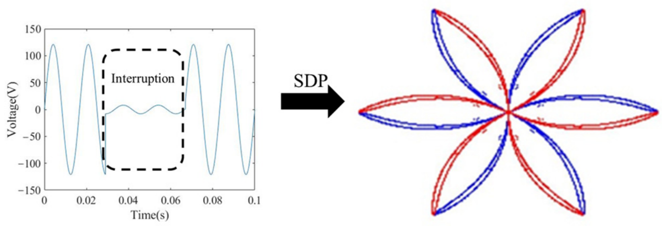

(**D**)

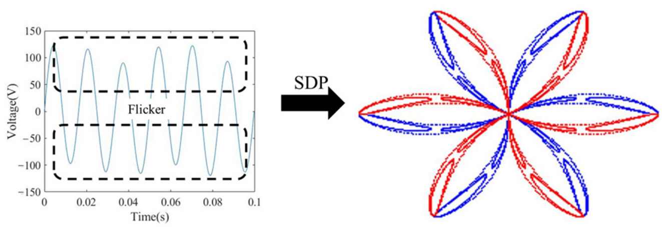

(**E**)

Figure 8. *Cont*.

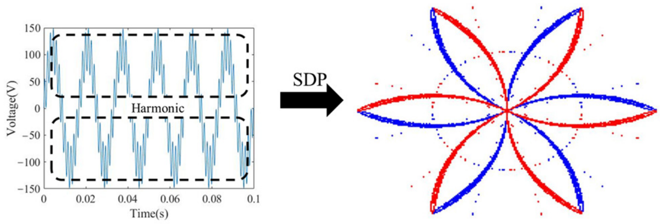

(**F**)

Figure 8. (**A**) Normal energy eigenvalue curve. (**B**) Sag energy eigenvalue curve. (**C**) Swell energy eigenvalue curve. (**D**) Interruption energy eigenvalue curve. (**E**) Flicker energy eigenvalue curve. (**F**) Harmonic energy eigenvalue curve.

5.3. CNN Recognition Result

CNN identified the eigenvalues of various accidents, and the result was compared with other recognition methods (HOG+SVM, HOG+Ensemble, and HOG+KNN). Table 1 shows the simulation results. The recognition accuracy of SDP+CNN is 94.2%, the accuracy of SDP+HOG+SVM is 89.0%, and the recognition rates of SDP+HOG+Ensemble and SDP+HOG+KNN are 85.4% and 84.4%, respectively. According to training time, the SDP+CNN needs 39 s, which is quite time-consuming with the highest test accuracy of 94.2% and 0.034 s for execution. The test environment was MATLAB 2020a, using an Intel® Core™ i5-10400 CPU@2.90 GHz processor, NVIDIA GeForce GTX 1660 SUPER graphics adapter, and Windows 10 professional 64-bit operating system.

Table 1. Test accuracy results of different methods.

Testing Method	Training Time (s)	Execution Time (s)	Test Accuracy
SDP+CNN	39	0.034	94.2%
SDP+HOG+SVM	3.1	0.012	89.0%
SDP+HOG+Ensemble	11.3	0.062	85.4%
SDP+HOG+KNN	7.0	0.008	84.4%

Figure 9 is the confusion matrix, which shows the recognition result of power quality. As seen, the x-axis is the fault type, and the y-axis is the predicted fault type. The numbers of accurate recognitions and misrecognitions are denoted by the green and red grids in the confusion matrix, respectively. The green and red values on the x-axis' light gray grids are the recognition accuracy and misrecognition rate of specific fault types, respectively. The green and red values in the lower rightmost dark gray grids are the overall recognition accuracy and misrecognition rates, respectively. The overall recognition accuracy can be obtained by dividing the total value of green grids by the total value of green and red grids. As shown in Figure 9, the proposed method identified 19 out of 20 test data as Interruption and misidentified only one as Swell. Therefore, the recognition rate of Interruption is 95%. Similarly, the recognition rates of Flicker, Harmonic, and Normal of the proposed method are all 100%, while the Sag and Swell recognition rates are 80% and 90%, respectively. Finally, the total recognition accuracy of 94.2% was obtained by dividing the total value of green grids by the total value of green and red grids.

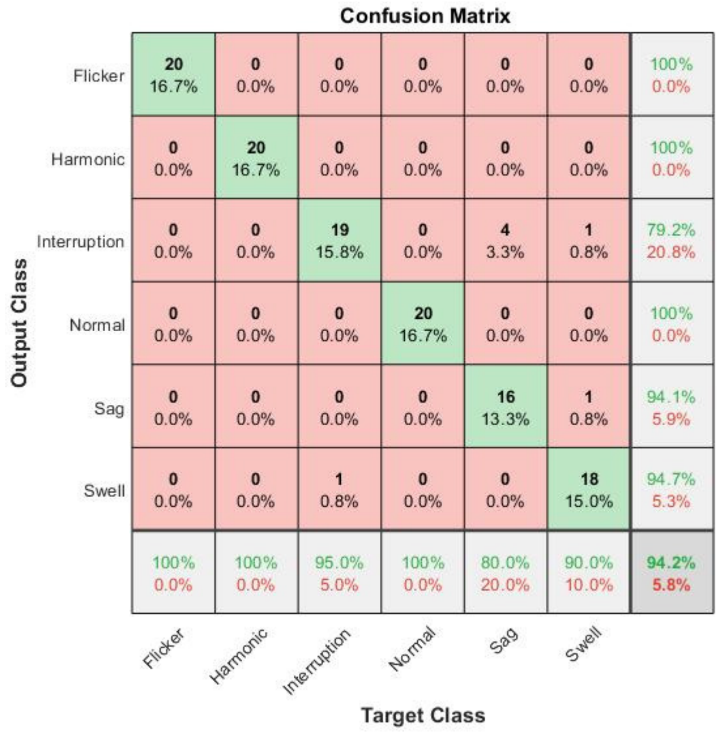

Figure 9. CNN resulting image.

6. Conclusions

Based on six constant fault models of power quality, this study proposed a power quality fault recognition method based on SDP and CNN. It can effectively identify the fault types, including voltage sag, voltage swell, voltage interruption, voltage harmonic, and voltage flicker. First, the signals were converted by SDP and imported into the CNN for recognition. The results indicate that the recognition rate of the proposed method reached 94.2%. The recognition accuracy was increased by almost 5% compared to other algorithms. Additional types of power quality events, such as voltage impulse, three-phase unbalance, and frequency drift, can be included in future research to construct power quality accident data signals more completely.

Author Contributions: Methodology, M.-H.W.; Validation, S.-H.C.; Resources, M.-H.W.; Writing—original draft, S.-H.C.; Writing—review & editing, S.-H.C.; Supervision, S.-D.L. All authors have read and agreed to the published version of the manuscript.

Funding: The authors gratefully acknowledge the financial support of the Ministry of Science and Technology of Taiwan, under contract number: MOST 110-2221-E-167-008-MY3.

Data Availability Statement: Data sharing not applicable.

Conflicts of Interest: The authors declare no conflict of interest.

References

1. Paul, S.; Dey, T.; Saha, P.; Dey, S.; Sen, R. Review on the development scenario of renewable energy in different country. In Proceedings of the 2021 Innovations in Energy Management and Renewable Resources(52042), Kolkata, India, 5–7 February 2021; pp. 1–2.
2. Şerban, A.C.; Lytras, M.D. Artificial Intelligence for Smart Renewable Energy Sector in Europe—Smart Energy Infrastructures for Next Generation Smart Cities. *IEEE Access* **2020**, *8*, 77364–77377. [CrossRef]
3. Wang, X.; Zhang, K. Cultivation of low-carbon design awareness in artificial intelligence era. In Proceedings of the 2010 International Conference on Artificial Intelligence and Education (ICAIE), Hangzhou, China, 29–30 October 2010; pp. 373–375.
4. Wang, H.; Liu, Y.; Wang, Z.; Du, B.X.; Pan, Z.; Liu, H.; Zong, H. Relationship Between Typical Defects of Power Cable Systems and the Harmonic Characteristics of Grounding Currents. In Proceedings of the 2022 IEEE 4th International Conference on Dielectrics (ICD), Palermo, Italy, 3–7 July 2022; pp. 750–753.

5. Devadasu, G.; Sushama, M. A novel multiple fault identification with fast Fourier transform analysis. In Proceedings of the 2016 International Conference on Emerging Trends in Engineering, Technology and Science (ICETETS), Pudukkottai, India, 24–26 February 2016.
6. Devadasu, G.; Sushama, M. Identification of voltage quality problems under different types of Sag/Swell faults with Fast Fourier Transform analysis. In Proceedings of the 2016 2nd International Conference on Advances in Electrical, Electronics, Information, Communication and Bio-Informatics (AEEICB), Chennai, India, 27–28 February 2016.
7. Zhang, P.; Feng, Q.; Chen, R.; Wang, D.; Ren, L. Classification and Identification of Power Quality in Distribution Network. In Proceedings of the 2020 5th International Conference on Power and Renewable Energy (ICPRE), Shanghai, China, 12–14 September 2020; pp. 533–537.
8. Radil, T.; Ramos, P.M.; Janeiro, F.M.; Serra, A.C. PQ Monitoring System for Real-Time Detection and Classification of Disturbances in a Single-Phase Power System. *IEEE Trans. Instrum. Meas.* **2008**, *57*, 1725–1733. [CrossRef]
9. Biletskiy, Y.; Chang, N.; Sharaf, A.M.; Mahasneh, H.A. A Monitoring and Identification Scheme for Power Quality Assessment. In Proceedings of the 2007 IEEE Canada Electrical Power Conference, Montreal, QC, Canada, 25–26 October 2007; pp. 520–524.
10. Silva, L.R.M.; Duque, C.A.; Ribeiro, P.F. Power Quality waveform recognition using Google Image Search Engine (iPQ-Google). In Proceedings of the 2016 17th International Conference on Harmonics and Quality of Power (ICHQP), Belo Horizonte, Brazil, 16–19 October 2016; pp. 1010–1013.
11. Chen, T.; Zhao, Y.; Li, T.; Luo, P.; Hou, Y.; Li, Z. Automatic identification of power quality signal of distribution network based on HHT and RVM. In Proceedings of the 2021 China International Conference on Electricity Distribution (CICED), Shanghai, China, 7–9 April 2021; pp. 111–114.
12. Han, Y.; Feng, Y.; Yang, P.; Xu, L.; Xu, Y.; Blaabjerg, F. Cause, Classification of Voltage Sag, and Voltage Sag Emulators and Applications: A Comprehensive Overview. *IEEE Access* **2020**, *8*, 1922–1934. [CrossRef]
13. Skolota, V.A.; Zinovev, G.S. Detecting Voltage Swell, Interruption and Sag. In Proceedings of the 2018 19th International Conference of Young Specialists on Micro/Nanotechnologies and Electron Devices (EDM), Erlagol, Russia, 29 June–3 July 2018; pp. 6403–6408.
14. Alarcón, C.M.; Rodríguez-Pajarón, P.; Bayo, A.H. Assessment of Flicker in a Low Voltage Residential Network. In Proceedings of the 2021 IEEE Madrid PowerTech, Madrid, Spain, 28 June–2 July 2021; pp. 1–6.
15. Nömm, J.; Rönnberg, S.; Bollen, M. Harmonic voltage measurements in a single house microgrid. In Proceedings of the 2018 18th International Conference on Harmonics and Quality of Power (ICHQP), Ljubljana, Slovenia, 13–16 May 2018; pp. 1–5.
16. Long, Z.; Zhang, X.; He, M.; Huang, S.; Qin, G.; Song, D.; Tang, Y.; Wu, G.; Liang, W.; Shao, H. Motor Fault Diagnosis Based on Scale Invariant Image Features. *IEEE Trans. Ind. Inform.* **2022**, *18*, 1605–1617. [CrossRef]
17. Long, Z.; Zhang, X.; Song, D.; Tang, Y.; Huang, S.; Liang, W. Motor Fault Diagnosis Using Image Visual Information and Bag of Words Model. *IEEE Sens. J.* **2021**, *21*, 21798–21807. [CrossRef]
18. Wang, H.; Xu, J.; Yan, R. Bearing Fault Diagnosis Based on Visual Symmetrized Dot Pattern and CNNs. In Proceedings of the 2019 IEEE International Instrumentation and Measurement Technology Conference (I2MTC), Auckland, New Zealand, 20–23 May 2019.
19. Li, Z.; Liu, Y.; An, J. Visualization of CNN Transient Voltage Classification Based on Feature Recognition and Enhancement. In Proceedings of the 2021 IEEE Sustainable Power and Energy Conference (iSPEC), Nanjing, China, 23–25 December 2021; pp. 3894–3899.
20. Yang, B.; Peng, X.; Liu, Y. Classification of Voltage Sag Sources Based on PCA-CNN-LVQ Method. In Proceedings of the 2021 IEEE Sustainable Power and Energy Conference (iSPEC), Nanjing, China, 23–25 December 2021; pp. 2337–2342.